Pontificia Universidad JAVERIANA Bogotá

Univ. Sci. 22 (3): 215-236, 2017.
doi: 10.11144/Javeriana.SC22-3.htcc

ORIGINAL ARTICLE

High temperature CO_2 capture of hydroxyapatite extracted from tilapia scales

Oscar H. Ojeda-Niño[1], Carolina Blanco[2], Carlos E. Daza[1,*]

Edited by
Juan Carlos Salcedo-Reyes
(salcedo.juan@javeriana.edu.co)

1. Estado Sólido y CatálisisAmbiental. Departamento de Química, Facultad de Ciencias, Universidad Nacional de Colombia, AK 30 No 45-03 Bogotá, D.C., Colombia,

2. Departamento de Química, Facultad de Ciencias, Universidad Nacional de Colombia, AK 30 No 45-03 Bogotá, D.C., Colombia.

* cedazav@unal.edu.co

Received: 28-06-2017
Accepted: 20-10-2017
Published on line: 25-11-2017

Citation: Ojeda-Niño O, Blanco C, Daza CE. High temperature CO_2 capture of hydroxyapatite extracted from tilapia scales, *Universitas Scientiarum*, 22 (3): 215-236, 2017. doi: 10.11144/Javeriana.SC22-2.htcc

Funding:
N/A

Electronic supplementary material:
N/A

Abstract

Hydroxyapatite (HAp) was obtained from tilapia scales by two extraction methods: direct calcination and acid-base treatment. The physicochemical characteristics of the obtained HAps were evaluated by thermogravimetric analysis, X-ray fluorescence, X-ray diffraction, scanning electron microscopy, surface area, infrared spectroscopy, and basicity measurement at 298 K by CO_2 -pulse titration. Furthermore, the CO_2 capture capacity of the solids at high temperature was also determined. Both methods showed the presence of a HAp phase although significant differences in the properties of the solids were found. The HAp obtained by direct calcination, exhibited a lower crystallinity and a greater surface area and basicity than the HAp obtained by the acid-base treatment. These features were correlated with the solid's CO_2 capture capacity. In this work, CO_2 capture capacity values for HAp yielded by calcination ranged from 2.5 to 3.2 mg CO_2 /g captured at 973 K, and for the acid-base treatment-derived HAp, CO_2 capture capacity values between 1.2 to 2.5 mg CO_2 /g were recorded. These results reveal the potential of HAps extracted from tilapia scales as solids with high CO_2 capture capacity, thermal stability, and capture/release cycles reversibility.

Keywords: fish scales; tilapia; hydroxyapatite; calcium; CO_2 capture

Introduction

Millions of tons of fish scales are discarded and wasted around the world. In Colombia, fish scales are considered worthless, unusable, and are often eliminated as waste. Consequently, the local fish industry generates large amounts of fish waste per year, of which tilapia scales have a considerable share. Ideas have been proposed on how to create value for fish scales and how to use this resource [1 - 4]. The surface of fish scales is constituted by numerous high-value organic and inorganic components, such as hydroxyapatite

(HAp) [5 - 7] and collagen [8, 9], both of them are of interest to the food manufacturing, cosmetics, functional biomedical product, and catalytic material industries.

Whereas collagen is highly valued in the industry due to its applications in cosmetic production, interest in HAp has grown for its uses as biomaterial [10, 11], adsorbent [12 - 14], and as catalytic reaction supporter [15 - 17]. HAp is commonly synthesized using wet methods or through solid state reactions to refine particle size or define a specific morphology. However, these methods can be costly and time-consuming, so their production from Ca-rich waste is of relevance from an industrial point of view. The HAp contained in fish scales is a crystallized form of calcium hydroxy-phosphate, and it can be easily extracted by thermal methods or acid treatment [18, 19].

There is currently great concern about the negative effects of global warming on the planet's climate. This climatic anomaly has its origin in the high accumulation of greenhouse gases such as CO_2 and CH_4, which are generated mainly by anthropogenic activities. In fact, the generation of energy from petroleum derivatives has significantly increased the concentrations of CO_2 in the atmosphere. Because of the magnitude of the effects of this gas on the environment, the reduction of CO_2 emissions is one of the great challenges of the century [20].

In order to reduce the harmful effects of CO_2 on the environment numerous research efforts have been focused on developing methods of adsorption [21 - 23], capture and controlled release [24 - 26], and in boosting the catalytic transformation of CO_2 into products of commercial interest [27 - 29]. Among these methods, that of CO_2 capture on oxide or Ca-compounds deserves special mention because CaO can form bulk carbonates which, by thermal decomposition, easily release CO_2 . This type of solids can be obtained from Ca-rich biological waste, like fish scales, and can be directed to form crystalline phases with high thermal stability such as HAp.

Several authors have reported the use of CaO-based solids to capture CO_2, and have provided evidence for the low thermal stability of CaO, because of the sintering of granules and destruction of the adsorbent porosity. Landi *et al*. [30], studied the formation of porous microgranules from a modified synthetic HAp, these solids capture CO_2 at temperatures between 800 °C and 1000 °C. They suggested that HAp can capture CO_2 through the formation of apatite carbonate ($Ca_{10}(PO_4)_6$ CO_3) inside the pores of HAp. Hap's weight increase

by CO_2 capture was 2.5 % w/w, showing high thermal stability during several carbonation-release cycles, as compared to CaO which showed low thermal stability.

Regarding the thermal stability of CaO, Xu *et al.* [31] evaluated the performance of Ni/CaO-Al_2O_3 as a bifunctional catalyst in capturing and releasing CO_2 , which they explained as a function of the decomposition of $CaCO_3$ into CaO at 800 °C and the carbonation of CaO into $CaCO_3$ at 650 °C. The CO_2 capture capacity of catalysts Ni/CaO, Ni/Al_2O_3 and Ni/CaO-Al_2O_3 was evaluated by varying the CaO/Al_2O_3 mass ratio. The Ni/CaO catalyst showed a higher CO_2 -capture capacity during the first cycles (0.5 g CO_2 /g), but after 10 cycles its capacity drastically dropped until reaching 0.25 g CO_2 /g, after 50 cycles, revealing its poor thermal stability for CaO. In contrast, the thermal stability of CaO-Al_2O_3 solids was significantly better, with a minimal loss of CO_2 capture capacity after 10 cycles. This stability was attributed to the formation of $Ca_5Al_6O_{14}$ species uniformly distributed in the catalyst, delaying the destruction of the CaO and $CaCO_3$ granules at high temperatures [32].

In addition, Cesário *et al.* [33] studied CaO-mayenite systems ($Ca_{12}Al_{14}O_{33}$), varying the CaO/$Ca_{12}Al_{14}O_{33}$ ratio and the synthesis method. Their results showed a CO_2 capture capacity of 0.43 g CO_2 /g, and that the presence of another phase different than CaO (*i.e.* $Ca_{12}Al_{14}O_{33}$) improved CO_2 capture. Martavaltzi *et al.* [34] evaluated CaO synthesized from thermal decomposition of $Ca(OH)_2$ and Ca $(CH_3COO)_2$. CaO from calcium acetate and obtained the best results with a weight increase of 0.5 g CO_2 /g in the first cycle, followed by a drastic dropping when the number of cycles increase. $Ca_{12}Al_{14}O_{33}$ was incorporated to improve thermal stability, providing a CO_2 capture capacity of 0.325 g CO_2 /g after 45 cycles. Furthermore, Castilho *et al.* [35] prepared various adsorbents for CO_2 -capture from biogenesis waste treated at 950 °C to decompose the different materials into CaO. Their results showed that samples with greater CO_2 capture capacity (0.25 g CO_2 /g) were those with higher surface area and porosity, smaller particle size, and lower micro-element traces associated with the starting materials.

In the present paper, we report the results of a physicochemical and morphological characterization of HAps obtained from red tilapia scales found in Colombian fish markets. Tilapia-derived HAps were synthesized following direct calcination and acid-base treatment methods. Thermogravimetric analysis, elemental analysis by X-ray fluorescence, X-ray diffraction, scanning electron microscopy, surface area, infrared spectroscopy, and basicity measurements by CO_2 -pulse titration at 298 K were used to

carry out a complete description of the characteristics of the tilapia-derived HAps. Since tilapia scales are a biological Ca source, the present investigation also explores the CO_2 capture and release capacities below 923 K for tilapia scale-derived HAps to study their potential use as low-cost adsorbents in mitigating atmospheric CO_2 loads.

Materials and methods

Hydroxyapatite (HAp) extraction

Red tilapia (*Oreochromis* sp.) scales used as raw material were collected in common commercialization sites from the Department of Huila (2.9345 °N, 75.2809° W) in Colombia (**Fig. 1**) Scales were washed with distilled water, dried at room temperature and triturated before use. HAp was extracted from the raw material by two methods as reported in the literature [18, 19]. According to method one, scales were directly calcined in static air at 973 K for 5 h with a ramp of 10 K min^{-1}.

As to method two, known as the acid-base treatment, the scales were deproteinized with 0.1 *M* HCl and washed with distilled water; subsequently, they were treated with 5 % w/v NaOH at 343 K for 5 h. After this time, the fine white precipitated powder was rinsed with distilled water and finally treated with 50 % w/v NaOH under reflux for 1 h. The final solid was washed, dried at 333 K, and calcined in static air at 973 K for 5 h with a ramp of 10 K min^{-1}.

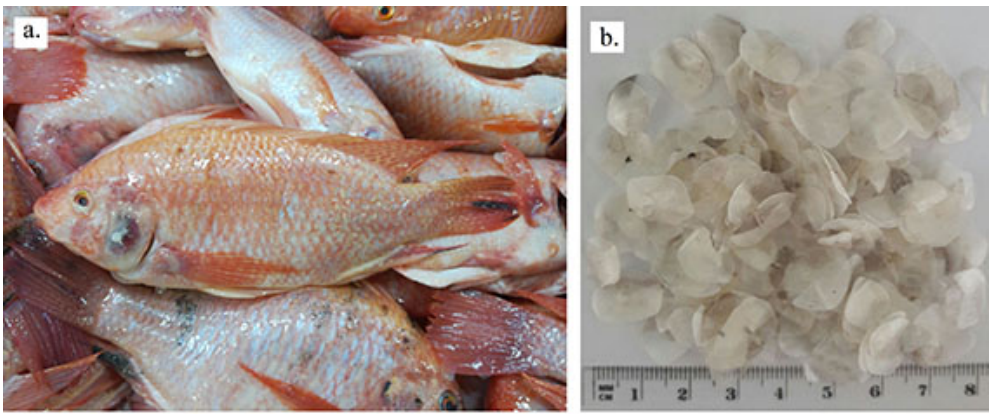

Figure 1. Pictures of **a**) Red tilapia as found in local fish markets and **b**) scales.

Characterization

Thermal decomposition of the raw material was examined by Thermogravimetric Analysis (TGA) and Differential Scanning Calorimetry (DSC) in air atmosphere of 80 % v/v N_2, 20 % v/v O_2. A TA-SDT-Q-600 apparatus (TA Instruments Corporate Headquarters, New Castle, UK) equipped with a TGA-DSC module was employed under a heating ramp of 10 $Kmin^{-1}$. An Al_2O_3 crucible was used as reference for the tests.

Elemental analysis was performed by X-ray fluorescence (XRF) on a PHILIPS PANALYTICAL MAGIXPRO PW-2440 (Nottingham, UK) spectrometer equipped with an Rh-tube. The sensitivity of this equipment is 0.02 % w/w. X-ray powder diffraction (XRD) profiles were taken on a PANALYTICAL XPERT PRO MPD (Almelo, The Netherlands) with 2θ geometry, using a Cu-anode ($\lambda = 0.154056$ nm) and step/time ratio of 0.02 $°2\theta s^{-1}$.

The morphology of the solids was observed by Scanning Electron Microscopy (SEM) using a TESCAN VEGA 3SB microscope (Brno, Czech Republic) that operates with a W-filament. For this analysis, samples were deposited on carbon tapes and coated with a gold layer prior to visualization.

The surface area of a studied sample was assessed by the Brunauer–Emmett Teller (B.E.T.) method ($0.05 \leq P/P^0 \leq 0.35$) entailing N_2-adsorption at 76 K using a MICROMERITICS ASAP 2020 equipment (Norcross, USA), with prior degassing under vacuum at 573 K for 4 h. The average particle diameter (D) was determined by **equation 1** referenced as in [2]:

$$D = \frac{6}{\rho S_{BET}} \tag{1}$$

Where D is the average particle size in μm, ρ is the density of pure HAp (3.16 gcm^{-3}), and S_{BET} is the B.E.T. surface area (m^2g^{-1}).

Fourier transform infrared spectroscopy (FTIR) analyses were conducted with a SHIMADZU IRTRACER-100 spectrometer (Kyoto, Japan). Samples were prepared as tablets by dilution with KBr.

Basicity measurements were carried out by CO_2 -chemisorption by pulses using a CHEMBET 3000 QUANTACHROME equipment (Boynton Beach, USA) following a method reported elsewhere [36].

Solids were previously degassed under He flow at 773 K for 1 h and the sample's CO_2 uptake was quantified using a thermal conductivity detector through injection pulses of 50 μL of CO_2 at 298 K [36].

CO_2 capture capacity measurements

In order to evaluate CO_2 capture capacity, a modified protocol was followed [32, 35], and it was conducted in a TGA equipment, model TA SDT Q 600 (TA Instruments Corporate Headquarters, New Castle, UK). A sample of 10 mg of HAp's with particle sizes less than 200 μm was placed in the microbalance of the TGA device and then heated to 1 073 K under N_2 atmosphere to ensure total decarbonation. Subsequently, the sample was subjected to 15 carbonation-decarbonation cycles, where a cycle consists of 15 min of carbonation at 923 K with pure CO_2 flow (50 mL min^{-1}) and 10 min of calcination at 1 073 K in N_2 (50 mL min^{-1}) with a heating and cooling rate of 10 K min^{-1}. The sample's CO_2 capture capacity, in mg CO_2/g of adsorbent, was calculated according to **equation 2**:

$$CO_2 \text{ capture capacity} = \frac{w_T - w_0}{w_0} \quad (2)$$

Where, w_t corresponds to the sample's weight at time t, and w_0 corresponds to its initial weight.

CO_2 capture capacity for bulk CaO was performed to establish a reference to which sample results could be compared. CaO was synthesized from $Ca(NO_3)_2.6H_2O$ calcined at 973 K for 5 h with a ramp of 10 K min^{-1}.

Results and Discussion

Fig. 2. illustrates the TGA and DSC profiles in air atmosphere of the raw material, namely tilapia scales thermal behavior. As revealed by its mass loss profile, at a temperature range of 300 to 500 K, there is an endothermic loss of 10.8 %, corresponding to a release of water and physisorbed gases. Subsequently there are two exothermic mass losses of 30.2 % between 500 and 600 K, and of 17.34 % loss between 600 and 800 K. The first exothermic event corresponds to thermal decomposition of organic macromolecules, while the second one corresponds to combustion of thermally stable molecular fragments and organic residues. The inorganic residue (ashes) obtained above 880 K, presumably HAp, constitutes 41.7 % of the initial mass.

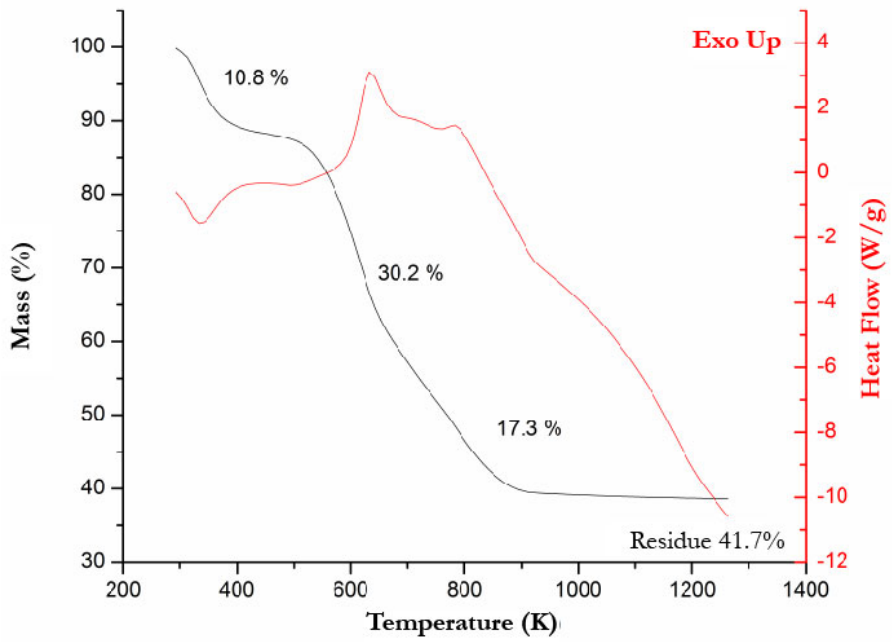

Figure 2. Thermogravimetric Analysis and Differential Calorimetry Scanning in air atmosphere for the raw material.

The absence of heat transfer or mass loss between 880 K and 1200 K suggests that the residue is thermally stable.

Since HAp synthesis of in this work was carried out by calcination at 973 K, a correct removal of organic compounds in the product after heat treatment should be assured. Additional TGA experiments performed on HAp extracted by both methods (not shown), revealed an endothermic mass loss of less than 3 % at temperatures below 200 K indicating an absence of organic residues.

Results of the elemental analysis performed on the HAp samples, reported as % w/w of the more stable oxides of the elements, are presented in **Table 1**. This analysis revealed that the most abundant elements are Ca and P, in a Ca/P molar ratio of 1.69 for HAp obtained by the calcination method; and that it is very close to the stoichiometric value of 1.67 of $Ca_{10}(PO_4)_6(OH)_2$. The acid-base treatment yielded HAp with a Ca/P molar ratio of 2.13, which is above the stoichiometric value. Such an observation agrees with P removal

Table 1. Elemental Analysis by X-ray Fluorescence for HAp samples.

Oxide	Calcination extracted (% weight)	Acid-base extracted (% weight)
CaO	55.39	59.77
P_2O_5	41.56	35.49
MgO	0.90	0.66
Na_2O	0.79	3.50
SO_3	0.62	0.04
SiO_2	0.24	0.33
Al_2O_3	0.09	0.04
Fe_2O_3	0.04	0.04
K_2O	0.04	0.02

during the acid-base treatment in the form of soluble phosphates, coupled with the decrease of S solubilized in the form of sulfates. These results can also be attributed to the exchange of phosphate ions by carbonate ions in the crystalline structure of HAp, as previously described in the literature [18, 35].

The analysis results in Table 1 also revealed the presence of elements such as Mg, Na, Si, Al, Fe, and K; these elements are typically found in biological material. Traces of Cu, Zn, and Sr, among others, were detected in HAp obtained by calcination and their presence was evidenced by the blue coloration of the sample. Such blue color was not observed in the Hap extracted by the acid-base treatment; because the elements responsible for this coloration are removed from the sample in the form of soluble salts. Consequently, the acid-base treatment lead to an increase in the Na concentration, with respect to the calcination method, due to the exchange of metal ions by Na^+ ions during the NaOH washes.

The XRD profiles for both the raw material (fish scales) and the obtained HAps are depicted in **Fig. 3**. The XRD for the scales (Fig. 3a) reveals the typical profile of a sample composed of both, crystalline and amorphous phases. Wide and low intensity signals in cps (counts per second) corresponding to the HAp phase, proteins and low crystalline polymeric carbohydrates, such as chitin and chitosan, belong to amorphous phases.

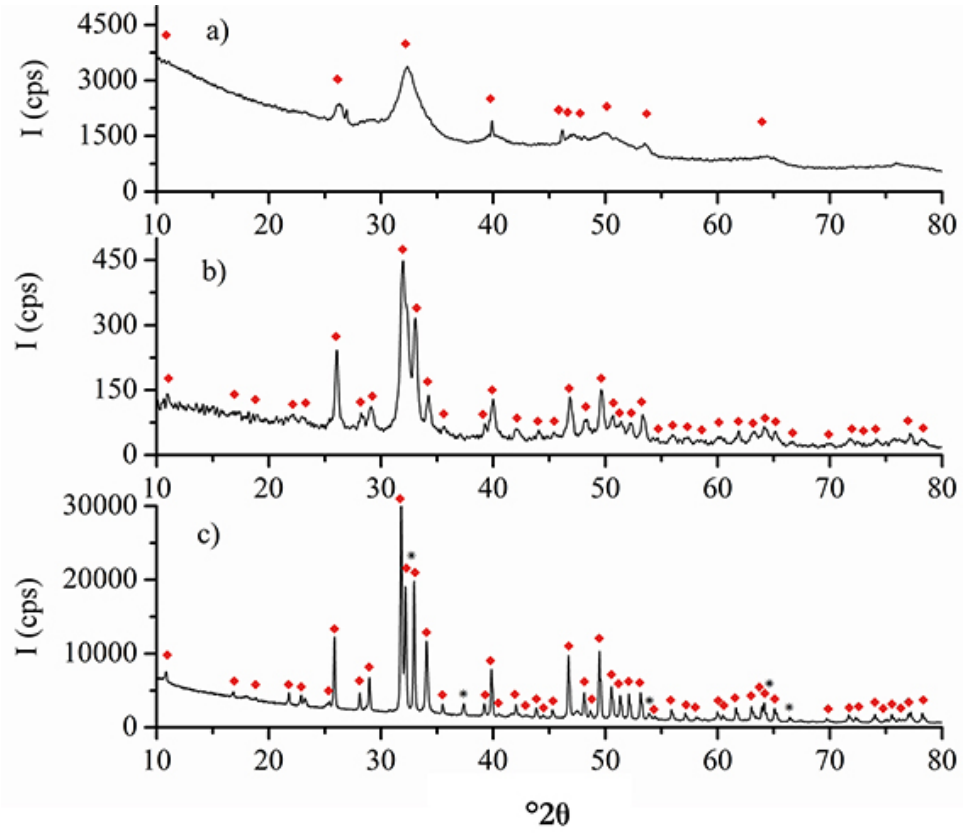

Figure 3. X-Ray Diffraction profiles for **a)** Raw material, **b)** HAp extracted by calcination and **c)** HAp extracted by acid-base treatment. ♦ HAp according to JCPDS 00-009-0432, * CaO according to JCPDS 00–082–1691.

The samples extracted by both treatments exhibited the typical XRD of an HAp phase, this was supported by the analysis results of the reference standard JCPDS 00-009-0432. Furthermore, these results are in accordance with the elemental analysis outcomes. However, the differences between the HAp obtained by the two methods are worth noting. The HAp that resulted from calcination (Fig. 3b), revealed a lower crystallinity than that of the HAp obtained by acid-base treatment (Fig. 3c), as more intense (in cps) and defined signals were obtained for the latter sample. In addition, HAp from the acid-base treatment, exhibited signals at 37.3, 53.9 and 66.5 °2θ corresponding to the CaO phase according to the results on the reference standard JCPDS 00-082-1691). The reason for this is the formation of CaO by solubilization and segregation of Ca from the HAp phase after treatment with strong acids and bases.

The low crystallinity of the HAp obtained by calcination suggests that heat treatment on the raw material hindered the formation of large HAp crystals due to the rapid decomposition of organic matter. In contrast, a gradual solubilization of proteins and carbohydrates, at places where small surface HAp crystals are embedded, occurred during the acid-base treatment. Thus, this method resulted in a gradual nucleation and growth of HAp.

To observe the surface morphology of the raw material and derived HAps, SEM micrographs were produced **(Fig. 4)**. The raw material (Fig. 4a) has a typical morphology of a biogenesis material, characterized by a heterogeneous, irregular surface with a series of intermixed fibers corresponding to the organic matrix of the hard tissues. The HAp obtained by calcination (Fig. 4b) has a heterogeneous morphology composed of intermixed granules with a flat surface, rough edges and different sizes; whereas, the HAp yielded by acid-base treatment (Fig. 4c) shows a fine flower-like morphology caused by a slow crystal growth; this is correlated with the high crystallinity evidenced in XRD for this sample.

The FTIR spectra for the samples are summarized in **Fig. 5**. The FTIR for the raw material (Fig. 5a) evidences a wide peak at 3 420 cm^{-1} corresponding to -O-H stretching vibrations of polymeric carbohydrates and overlapped stretching bands of -N-H groups in the collagen; and a wide and intense peak at 2 960 cm^{-1}, corresponding to -C-H stretches belonging to carbon skeletons. Furthermore, the raw material also exhibits peaks at 1 654 and 1 545 cm^{-1}, assigned to type-I and -II amide (typical of samples containing collagen); peaks at 1 440 and 871 cm^{-1},assigned to asymmetrical and out-of-plane stretching CO_3^{2-}; and a peak at 1 026 cm^{-1}, corresponding to P-O stretches in PO_4^{3-} [5, 19].

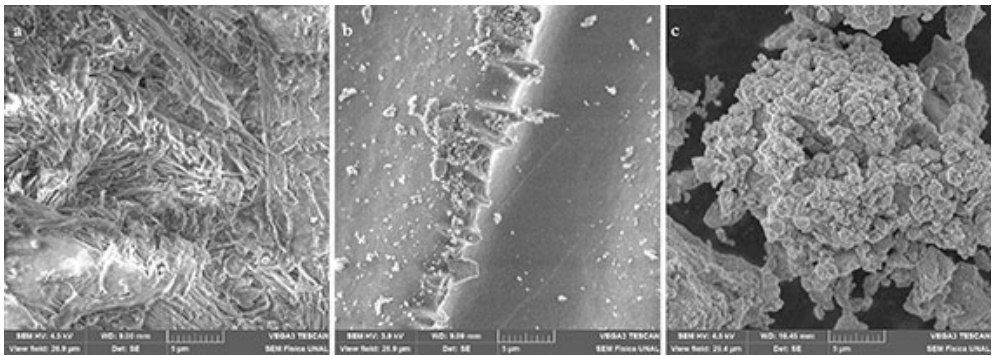

Figure 4. Scanning Electron Microscopy for raw material **a)**, HAp extracted by calcination **b)** and HAp extracted by acid-base treatment **c)**.

The FTIR spectra for HAp obtained by direct calcination (Fig. 5b) and acid-base treatment (Fig. 5c) lacked the signals found in the raw material; consequence of the elimination of organic compounds, such as collagen. The peaks at 3 566, 3 580, 3 466, and 3 418 cm^{-1} correspond to -O-H groups stretching vibrations. The shape and intensity of these signals are typical of an HAp phase [19].

The peak at 1 470 cm^{-1} in (Fig. 5b) corresponds to a symmetric stretching of CO_3^{2-}, this signal is more pronounced in the HAp prepared by acid–base treatment (precisely at 1 475 cm^{-1}, (Fig. 5c). According to XRD results, the HAp obtained by acid-base treatment contains CaO, (see Fig. 3); CaO can be easily carbonated to give $CaCO_3$. The intense and wide peaks, ranging between 1 000 cm^{-1} and 1 100 cm^{-1}, as well as the peaks around 595 cm^{-1} relate to the different types of stretches of the P–O bond in PO_4^{2-} (Fig. 5b and 5c). The FTIR spectra of these materials are very similar to those reported for HAp from other types of fish scales, confirming the effective extraction of both methods [2, 6].

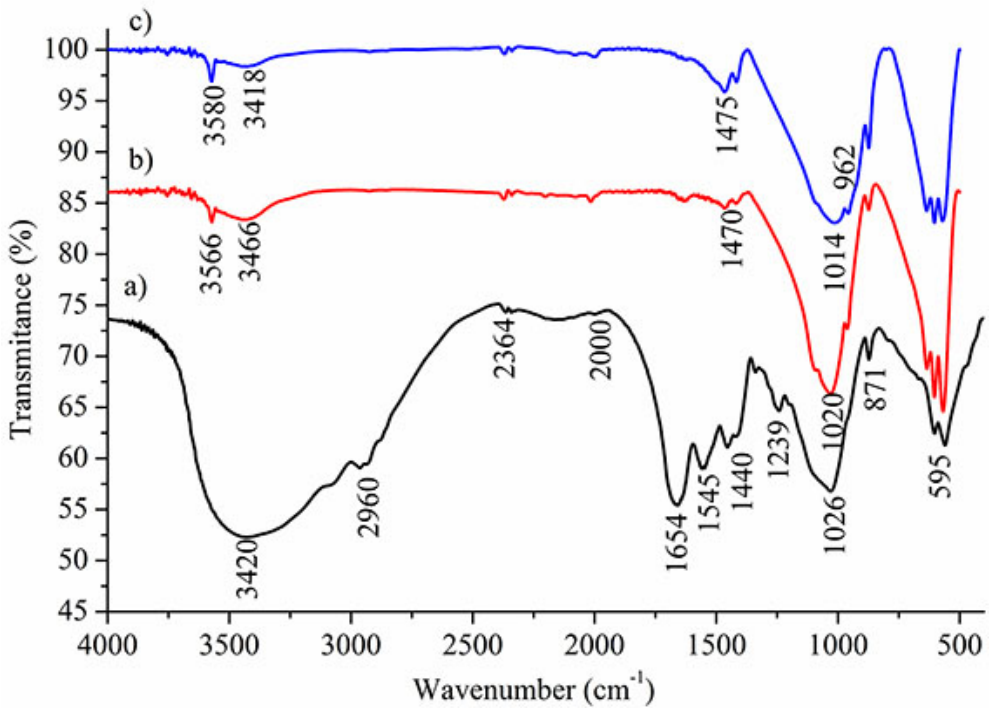

Figure 5. FTIR spectra for **a)** Raw material, **b)** HAp extracted by calcination and **c)** HAp extracted by acid-base treatment.

The B.E.T. area values registered for the obtained HAp samples are given in **Table 2**. The surface areas are particularly low (17.5 and 2.5 m^2g^{-1}), compared to the reported value from commercial HAp of 56.8 m^2g^{-1} [2]. This HAp ha a low porosity in consonance with the type of morphology observed in the SEM micrographs in Fig. 4, showing compact and poorly porous granules. Contrastingly, the HAp obtained by calcination has a higher surface area because of its lower crystallinity and particle size. The average calculated particle sizes were 0.108 μm for HAp (calcination) and 0.759 μm for HAp (acid-base treatment).

The basicity analysis results of the obtained HAps are presented in Table 2. These analyses were based on CO_2 -pulse titration at 298 K, and their results expressed as μmol/g and μmol/m^2 of CO_2 uptake Compared with other types of solids, such as MgO [37], CaO [38], or Mg-Al mixed oxides [39], which have basicities as high as 180 μmol/g, the basicity of the studied HAps is considerably low, indicating that these solids have a moderate surface basicity, and that they mainly have surface sites where physisorption mechanisms occur through formation of surface carbonates [36]. The present analysis results are correlated with those of B.E.T areas, crystal size and crystallinity, all leading to the conclusion that basicity increases with increasing area and decreasing crystal size.

To establish whether HAp from tilapia scales retain any CO_2 capture capacity at high temperature, thermogravimetric experiments were carried out through 15 carbonation-decarbonation cycles (**Fig. 6**). The CO_2 capture mechanism on Ca-containing solids has been reported in the literature [40]. In the first stage, the pores of the adsorbent are rapidly filled by CO_2 forming a layer of surface $CaCO_3$, subsequently CO_2 molecules diffuse from the surface layer into granules in a stage governed by a diffusional regime. This mechanism is desired because it allows for the adsorbent to be easily regenerated after saturation. Then, in the calcination step, or second stage, the adsorbent partially or totally releases CO_2 from the pores through a diffusive process, which happens at high temperature because of the strong interaction. There is evidence that total CO_2 release happens between 700 °C and 750 °C [35].

As can be seen in Fig. 6a, HAp obtained by acid – base treatment displays an initial CO_2 –capture capacity of 3.9 mg CO_2 /g, which decreases in the following cycles revealing a range of thermal stability from cycle two onwards with CO_2 –capture capacities fluctuating between1.2 and 2.5 mg CO_2 /g.

Table 2. B.E.T area and basicity by CO_2-pulse titration at 298 K for HAp samples.

HAp	B.E.T. area (m^2g^{-1})	CO_2-uptake	
		µmol/g	µmol/m^2
Calcination extracted	17.5	17.7	1.01
Acid-base extracted	2.5	1.3	0.52

Fig. 6b reveals that HAp obtained via calcination has a CO_2 capture capacity ranging between 2.5 mg and 3.2 mg CO_2 /g. CO_2 capture for this latter solid shows greater stability in all cycles without sudden losses and its CO_2 capture capacity and thermal stability increased when surface area and basicity were also higher.

The CO_2 capture capacity for bulk CaO is presented in Fig. 6c. CaO is expected to be a good adsorbent for CO_2 because it can form $CaCO_3$ stoichiometrically in a 1:1 ratio (**Equation 3**). As shown in **Fig. 6c** an initial capture capacity of 550 mg CO_2 /g was achieved, and it progressively decreased through the cycles down to a capture capacity of 200 mg CO_2 /g in cycle 15. The observed progressive decline is attributed to CaO-sintering and to the saturation of CO_2 forming surface $CaCO_3$ blocking the external pores of the solid.

CO_2 capture capacities of tilapia-scale-derived HAps are markedly lower than those for (synthetic) bulk CaO. Nevertheless, the results are promising because the observed CO_2 capture capacity values are of constant magnitudes, as it has been reported for synthetic HAp [30], and for $CaO/CaCO_3$–based solids extracted from Ca-rich food wastes [35]. Unlike the results for bulk CaO, the CO_2 capture capacity of the HAp obtained by calcination was not altered as cycles progressed, indicating that this solid is thermally stable. The calcination method is simple, inexpensive and does not involve the use of Al compounds to increase thermal stability [32-34].

The low CO_2 capture capacities for HAp, may be explained by the fact that the HAp phase cannot easily form bulk carbonates due to its structural crystallinity and thermal stability. In the HAp structure, the possible carbonate (apatite carbonate) route of formation is presented in **Equation 4** [30].

In this reaction, a dehydroxylation of the structure must occur to allow carbonate formation. However, TGA in Fig. 2 showed that the dehydroxylation of extracted HAp does not occur before 1 273 K, this suggests that the CO_2 capture capacity registered for HAp are mainly the product of the formation of surface $CaCO_3$ (not bulk). CO_2 diffusion towards the internal pores of the material is limited because of crystallinity of the HAp phase.

$$CaO_{(s)} + CO_{2(g)} \rightarrow CaCO_{3(s)} \quad (3)$$

$$Ca_{10}(PO_4)_6(OH)_{2(s)} + CO_{2(g)} \rightarrow Ca_{10}(PO_4)_6CO_3(s) + H_2O_{(g)} \quad (4)$$

A total reversibility in CO_2 capture–release cycles for the obtained Haps was observed (Fig. 6a and 6b). This opens the possibility for these inexpensive solids to be employed in the reuse of CO_2 captured from the atmosphere, through a controlled thermal release from the solid.

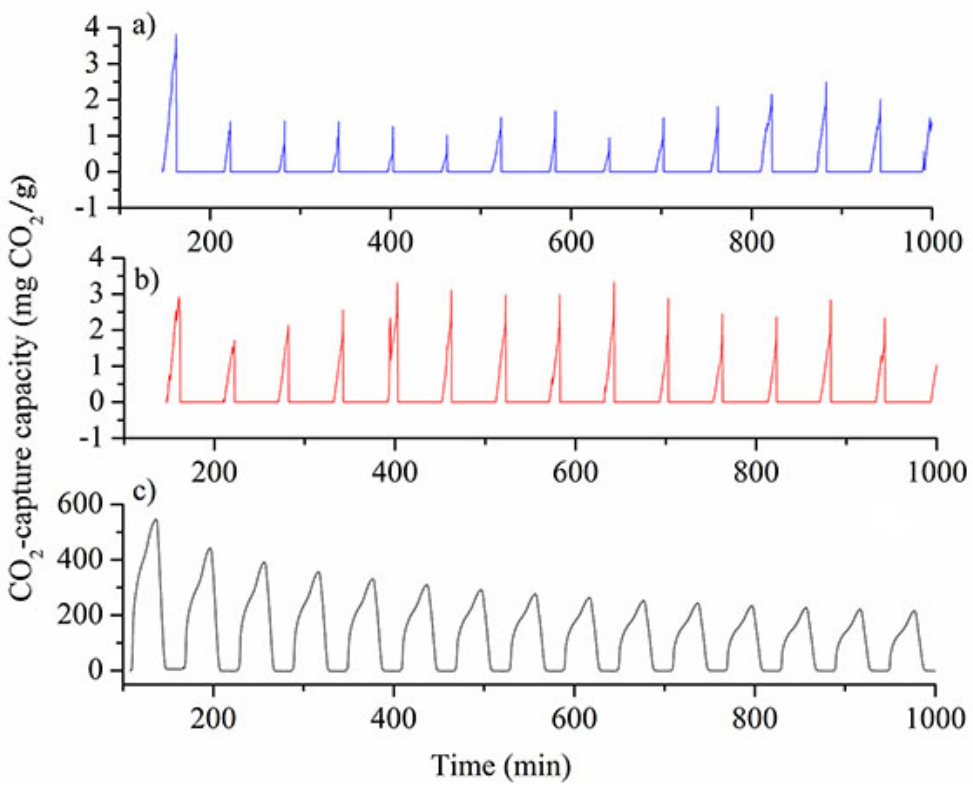

Figure 6. CO_2 capture capacity measurements for: **a)** HAp extracted by acid-base treatment, **b)** HAp extracted by calcination and **c)** bulk CaO.

Conclusions

Tilapia scales are a Ca-rich biogenesis waste with an inorganic residue of 41.68 % w/w. Hydroxyapatites were synthesized from tilapia scales by two methods: calcination and acid-base treatment. The HAps obtained by the two methods displayed different characteristics in their crystallinity, morphology, composition, surface area and basicity. HAp derived from direct calcination had lower crystallinity, lower grain size, and higher surface area than the HAp provided by acid base treatment, which correlated with a higher surface basicity. CO_2 capture capacities of the HAps were consequence of the formation of surface carbonates, finding values between 2.5 mg and 3.2 mg CO_2 /g for the HAp obtained by calcination, and 1.2 mg and 2.5 mg CO_2 /g for the HAp obtained by acid-base treatment that correlated with the basicity of solids. CO_2 capture capacity ranges reported here are promising for CO_2 capture solids at high temperature from biological sources, because their high thermal stability and reversibility in the capture/release detected.

Acknowledgments

Oscar H. Ojeda-Niño acknowledges COLCIENCIAS for the funding received as part of the Jóvenes Investigadores program, in the year 2015.

Conflict of interest

The authors of this manuscript have no conflict of interests to declare.

References

[1] Marrakchi F, Ahmed MJ, Khanday WA, Asif M, Hameed BH. Mesoporous carbonaceous material from fish scales as low-cost adsorbent for reactive orange 16 adsorption, *Journal of the Taiwan Institute of Chemical Engineers*, 71: 47-54, 2017.
doi: 10.1016/j.jtice.2016.12.026

[2] Muhammad N, Gao Y, Iqbal F, Ahmad P, Ge R, Nishan U, Rahim A, Gonfa G, Ullah Z. Extraction of biocompatible hydroxyapatite from fish scales using novel approach of ionic liquid pretreatment, *Separation and Purification Technology*, 161: 129-135, 2016.
doi: 10.1016/j.seppur.2016.01.047

[3] Prasad A, Mohan Bhasney S, Sankar MR, Katiyar V. Fish Scale Derived Hydroxyapatite reinforced Poly (Lactic acid) Polymeric Bio-films: Possibilities for Sealing/locking the Internal Fixation Devices, *Materials Today: Proceedings*, 4: 1340-1349, 2017.
doi: 10.1016/j.matpr.2017.01.155

[4] Sinha T, Ahmaruzzaman M, Sil AK, Bhattacharjee A. Biomimetic synthesis of silver nanoparticles using the fish scales of Labeo rohita and their application as catalysts for the reduction of aromatic nitro compounds, *Spectrochimica Acta Part A: Molecular and Biomolecular Spectroscopy*, 131: 413-423, 2014.

doi: 10.1016/j.saa.2014.04.065

[5] Mondal B, Mondal S, Mondal A, Mandal N. Fish scale derived hydroxyapatite scaffold for bone tissue engineering, *Materials Characterization*, 121: 112-124, 2016.

doi: 10.1016/j.matchar.2016.09.034

[6] Pon-On W, Suntornsaratoon P, Charoenphandhu N, Thongbunchoo J, Krishnamra N, Tang IM. Hydroxyapatite from fish scale for potential use as bone scaffold or regenerative material, *Materials Science and Engineering: C*, 62: 183-189, 2016.

doi: 10.1016/j.msec.2016.01.051

[7] Gunduz O, Kilic O, Ekren N, Gokce H, Kalkandelen C, Oktar FN. Natural Hydroxyapatite Synthesis from Fish Bones: "Atlantic Bonito" (Sarda sarda), *Key Engineering Materials*, 720: 207-209, 2016.

doi: 10.4028/www.scientific.net/KEM.720.207

[8] Chen J, Li L, Yi R, Xu N, Gao R, Hong B. Extraction and characterization of acid-soluble collagen from scales and skin of tilapia (Oreochromis niloticus), *LWT - Food Science and Technology*, 66: 453-459, 2016.

doi: 10.1016/j.lwt.2015.10.070

[9] Chen S, Chen H, Xie Q, Hong B, Chen J, Hua F, Bai K, He J, Yi R, Wu H. Rapid isolation of high purity pepsin-soluble type I collagen from scales of red drum fish (Sciaenops ocellatus), *Food Hydrocolloids*, 52: 468-477, 2016.

doi: 10.1016/j.foodhyd.2015.07.027

[10] Shi F, Zhi W, Liu Y, Zhou T, Weng J. One-step method to construct hydroxyapatite scaffolds with 3-D interconnected structure by a novel hydrogel bead porogen process, *Materials Letters*, 203: 13-16, 2017.

doi: 10.1016/j.matlet.2017.05.099

[11] Zheng X, Hui J, Li H, Zhu C, Hua X, Ma H, Fan D. Fabrication of novel biodegradable porous bone scaffolds based on amphiphilic hydroxyapatite nanorods, *Materials Science and Engineering: C*, 75: 699-705, 2017.

doi: 10.1016/j.msec.2017.02.103

[12] Ramakrishnan P, Nagarajan S, Thiruvenkatam V, Palanisami T, Naidu R, Mallavarapu M, Rajendran S. Cation doped hydroxyapatite nanoparticles enhance strontium adsorption from aqueous system: A comparative study with and without calcination, *Applied Clay Science*, 134, Part 2: 136-144, 2016.

doi: 10.1016/j.clay.2016.09.022

[13] Sarda S, Errassifi F, Marsan O, Geffre A, Trumel C, Drouet C. Adsorption of tranexamic acid on hydroxyapatite: Toward the development of biomaterials with local hemostatic activity, *Materials Science and Engineering: C*, 66: 1-7, 2016.

doi: 10.1016/j.msec.2016.04.032

[14] Scudeller LA, Mavropoulos E, Tanaka MN, Costa AM, Braga CAC, López EO, Mello A, Rossi AM. Effects on insulin adsorption due to zinc and strontium substitution in hydroxyapatite, *Materials Science and Engineering: C*, 79: 802-811, 2017.

doi: 10.1016/j.msec.2017.05.061

[15] Rêgo De Vasconcelos B, Zhao L, Sharrock P, Nzihou A, Pham Minh D. Catalytic transformation of carbon dioxide and methane into syngas over ruthenium and platinum supported hydroxyapatites, *Applied Surface Science*, 390: 141-156, 2016.

doi: 10.1016/j.apsusc.2016.08.077

[16] Boukha Z, Ayastuy JL, González-Velasco JR, Gutiérrez-Ortiz MA. CO elimination processes over promoter-free hydroxyapatite supported palladium catalysts, *Applied Catalysis B: Environmental*, 201: 189-201, 2017.

doi: 10.1016/j.apcatb.2016.08.039

[17] Boukha Z, Kacimi M, Pereira MFR, Faria JL, Figueiredo JL, Ziyad M. Methane dry reforming on Ni loaded hydroxyapatite and fluoroapatite, *Applied Catalysis A: General*, 317: 299-309, 2007.

doi: 10.1016/j.apcata.2006.10.029

[18] Chakraborty R, Bepari S, Banerjee A. Application of calcined waste fish (Labeo rohita) scale as low-cost heterogeneous catalyst for biodiesel synthesis, *Bioresource Technology*, 102: 3610-3618, 2011.

doi: 10.1016/j.biortech.2010.10.123

[19] Kongsri S, Janpradit K, Buapa K, Techawongstien S, Chanthai S. Nanocrystalline hydroxyapatite from fish scale waste: Preparation, characterization and application for selenium adsorption in aqueous solution, *Chemical Engineering Journal*, 215-216: 522-532, 2013.

doi: 10.1016/j.cej.2012.11.054

[20] Foster GL, Royer DL, Lunt DJ. Future climate forcing potentially without precedent in the last 420 million years, *Nature Communications*, 8: 14845-14853, 2017.

doi: 10.1038/ncomms14845

[21] Ammendola P, Raganati F, Chirone R. CO_2 adsorption on a fine activated carbon in a sound assisted fluidized bed: Thermodynamics and kinetics, *Chemical Engineering Journal*, 322: 302-313, 2017.

doi: 10.1016/j.cej.2017.04.037

[22] Chanapattharapol KC, Krachuamram S, Youngme S. Study of CO_2 adsorption on iron oxide doped MCM-41, *Microporous and Mesoporous Materials*, 245: 8-15, 2017.

doi: 10.1016/j.micromeso.2017.02.072

[23] Girimonte R, Formisani B, Testa F. Adsorption of CO_2 on a confined fluidized bed of pelletized 13X zeolite, *Powder Technology*, 311: 9-17, 2017.

doi: 10.1016/j.powtec.2017.01.033

[24] Irani M, Jacobson AT, Gasem KAM, Fan M. Modified carbon nanotubes/tetraethylenepentamine for CO_2 capture, *Fuel*, 206: 10-18, 2017.

doi: 10.1016/j.fuel.2017.05.087

[25] Slostowski C, Marre S, Dagault P, Babot O, Toupance T, Aymonier C. CeO2 nanopowders as solid sorbents for efficient CO_2 capture/release processes, *Journal of CO_2 Utilization*, 20: 52-58, 2017.

doi: 10.1016/j.jcou.2017.03.023

[26] Wang P, Guo Y, Zhao C, Yan J, Lu P. Biomass derived wood ash with amine modification for post-combustion CO_2 capture, *Applied Energy*, 201: 34-44, 2017.

doi: 10.1016/j.apenergy.2017.05.096

[27] Daza CE, Cabrera CR, Moreno S, Molina R. Syngas production from CO_2 reforming of methane using Ce-doped Ni-catalysts obtained from hydrotalcites by reconstruction method, *Applied Catalysis A: General*, 378: 125-133, 2010.

doi: 10.1016/j.apcata.2010.01.037

[28] Daza CE, Gallego J, Moreno JA, Mondragón F, Moreno S, Molina R. CO_2 reforming of methane over Ni/Mg/Al/Ce mixed oxides, *Catalysis Today*, 133–135: 357-366, 2008.

doi: 10.1016/j.cattod.2007.12.081

[29] Daza CE, Moreno S, Molina R. Co-precipitated Ni–Mg–Al catalysts containing Ce for CO_2 reforming of methane, *International Journal of Hydrogen Energy*, 36: 3886-3894, 2011.

doi: 10.1016/j.ijhydene.2010.12.082

[30] Landi E, Riccobelli S, Sangiorgi N, Sanson A, Doghieri F, Miccio F. Porous apatites as novel high temperature sorbents for carbon dioxide, *Chemical Engineering Journal*, 254: 586-596, 2014.

doi: 10.1016/j.cej.2014.05.070

[31] Xu P, Zhou Z, Zhao C, Cheng Z. Ni/CaO-Al_2O_3 bifunctional catalysts for sorption-enhanced steam methane reforming, *AIChE Journal*, 60: 3547-3556, 2014.

doi: 10.1002/aic.14543

[32] Xu P, Zhou Z, Zhao C, Cheng Z. Catalytic performance of Ni/CaO-$Ca_5Al_6O_{14}$ bifunctional catalyst extrudate in sorption-enhanced steam methane reforming, *Catalysis Today*, 259, Part 2: 347-353, 2016.

doi: 10.1016/j.cattod.2015.05.026

[33] Cesário MR, Barros BS, Courson C, Melo DMA, Kiennemann A. Catalytic performances of Ni–CaO–mayenite in CO_2 sorption enhanced steam methane reforming, *Fuel Processing Technology*, 131: 247-253, 2015.

doi: 10.1016/j.fuproc.2014.11.028

[34] Martavaltzi CS, Lemonidou AA. Development of new CaO based sorbent materials for CO_2 removal at high temperature, *Microporous and Mesoporous Materials*, 110: 119-127, 2008.

doi: 10.1016/j.micromeso.2007.10.006

[35] Castilho S, Kiennemann A, Costa Pereira MF, Soares Dias AP. Sorbents for CO_2 capture from biogenesis calcium wastes, *Chemical Engineering Journal*, 226: 146-153, 2013.

doi: 10.1016/j.cej.2013.04.017

[36] Daza CE, Gallego J, Mondragón F, Moreno S, Molina R. High stability of Ce-promoted Ni/Mg–Al catalysts derived from hydrotalcites in dry reforming of methane, *Fuel*, 89: 592-603, 2010.

doi: 10.1016/j.fuel.2009.10.010

[37] Chen A, Yu Y, Li Y, Li Y, Jia M. Solid-state grinding synthesis of ordered mesoporous MgO/carbon spheres composites for CO_2 capture, *Materials Letters,* 164: 520-523, 2016.

doi: 10.1016/j.matlet.2015.11.043

[38] Sengupta S, Deo G. Modifying alumina with CaO or MgO in supported Ni and Ni–Co catalysts and its effect on dry reforming of CH4, *Journal of CO_2 Utilization*, 10: 67-77, 2015.

doi: 10.1016/j.jcou.2015.04.003

[39] Hájek M, Kutálek P, Smoláková L, Troppová I, Čapek L, Kubička D, Kocík J, Thanh DN. Transesterification of rapeseed oil by Mg–Al mixed oxides with various Mg/Al molar ratio, *Chemical Engineering Journal*, 263: 160-167, 2015.

doi: 10.1016/j.cej.2014.11.006

[40] Zamboni I, Courson C, Niznansky D, Kiennemann A. Simultaneous catalytic H2 production and CO_2 capture in steam reforming of toluene as tar model compound from biomass gasification, *Applied Catalysis B: Environmental*, 145: 63-72, 2014.

doi: 10.1016/j.apcatb.2013.02.046

Captura de CO_2 a altas temperaturas, de hidroxiapatitas extraídas de escamas de tilapia

Resumen. Se obtuvo hidroxiapatita (HAp) de escamas de tilapia por dos métodos de extracción: calcinación directa y tratamiento ácido-base. Las características fisicoquímicas de las HAps obtenidas fueron evaluadas por análisis termogravimétrico, fluorescencia de rayos X, difracción de rayos X, microscopía electrónica de barrido, área superficial, espectroscopía infrarroja y medición de basicidad a 298 K por titulación por pulso de CO_2. Adicionalmente, se determinó la capacidad de captura de CO_2 de los sólidos a alta temperatura. Ambos métodos mostraron la presencia de una fase de HAp, aunque se encontraron diferencias significativas en las propiedades de los sólidos. La HAp obtenida por calcinación directa exhibió una menor cristalinidad y una mayor área superficial y basicidad que la HAp obtenida con el tratamiento acido-base. Estas características se correlacionaron con la capacidad de captura de CO_2 del sólido. En este trabajo, los valores de captura del CO_2 con la HAp producidos por calcinación oscilaron entre 2.5 to 3.2 mg CO_2/g capturado a 973 K, y con la HAp derivada del tratamiento ácido-base, se registraron valores de captura entre 1.2 to 2.5 mg CO_2/g. Estos resultados revelan el potencial de HAps extraídos de escamas de tilapia como sólidos con una alta capacidad de captura de CO_2, estabilidad térmica y reversibilidad de los ciclos de captura/liberación.

Palabras clave: escamas de pescado; tilapia, hidroxiapatita; CO_2 captura; calcio

Captura de CO_2 a altas temperaturas por hidroxiapatita extraída de escamas de tilápia

Resumo. A hidroxiapatita (HAp) foi obtida a partir da escama de tilápia usando dois métodos de extração: calcinação direta e tratamento ácido-base. As características físico-químicas das hidroxiapatitas foram avaliadas por análise termogravimétrica, fluorescência de raios-X, difração de raios-X, microscopia eletrônica de varredura, área superficial, espectroscopia de infravermelho e medição de basicidade a 298 K por titulação de pulso de CO_2. Além disso, determinou-se a capacidade de captura de CO_2 dos sólidos a alta temperatura. Os dois métodos mostraram a presença da fase HAp, no entanto, diferenças significativas foram encontradas nas propriedades dos sólidos, sendo a HAp obtida por calcinação direta a que apresentou menor cristalinidade, maior área superficial e basicidade, características que foram correlacionadas com a capacidade de captura de CO_2. Foram encontrados valores entre 2.5 a 3.2 mg CO_2/g capturado a 973 K para a HAp obtida por calcinação e, entre 1.2 a 2.5 mg CO_2/g para a HAp obtida por tratamento ácido-base. Isto revelou o potencial de HAp's extraídas da escama de tilapia como sólidos com alta capacidade de captura de CO_2, estabilidade térmica e reversibilidade na liberação de CO_2.

Palavras-chave: Escamas de tilápia; tilápia; hidroxiapatita; captura de CO_2; cálcio

Oscar H. Ojeda-Niño

Chemical Engineer, completed his undergraduate studies at Universidad Industrial de Santander and is currently a Master of Science student at Universidad Nacional de Colombia (Bogota D.C.-Colombia). Since his undergraduate studies, Oscar has been working in the field of catalysis, evaluating and designing catalytic materials aimed at solving environmental problems. In 2015 Oscar was recipient of the "Joven Investigador" research grant by COLCIENCIAS for the 2015-2016 period.

Carolina Blanco

Chemist graduated from Universidad Nacional de Colombia and received her M.Sc. and Ph.D. degrees, for her research in Homogeneous Catalysis, from Universitat Rovira i Virgili, Spain. Carolina conducted postdoctoral research at the Institute of Chemical Research of Catalonia, where she worked on metal catalyzed functionalization for transformations of alkenes. Since 2014, Carolina is Professor of Chemistry Department at Universidad Nacional de Colombia. Her current research interests include homogeneous catalysis for the synthesis of organic compounds from renewable sources, with a focus on the conversion of CO_2 to valuable products.

Carlos E. Daza

Chemist and Ph.D. in Chemistry, Carlos completed his degrees at Universidad Nacional de Colombia in Bogota and is currently Associate Professor of the Chemistry Department at Universidad Nacional de Colombia (Bogota D.C.-Colombia). and awarded COLCIENCIAS' senior researcher. Carlos research filed deals with chemical adsorbents and catalysts for reactions with heterogeneous beneficial impact on the environment, and his interest focuses on obtaining low-cost solids using agro-industrial waste and minerals as precursors.